Biochemical and Biophysical Research Communications 462 (2015) 1–7

Contents lists available at ScienceDirect

Biochemical and Biophysical Research Communications

journal homepage: www.elsevier.com/locate/ybbrc

Crystal structure of GnsA from *Escherichia coli*

Yong Wei [a, c, 1], Lihong Zhan [a, b, 1], Zengqiang Gao [b], Gilbert G. Privé [c, d, *], Yuhui Dong [b, **]

[a] School of Life Science, University of Science and Technology of China, Hefei 230027, China
[b] Beijing Synchrotron Radiation Facility, Institute of High Energy Physics, Chinese Academy of Sciences, Beijing 100049, China
[c] Department of Medical Biophysics, University of Toronto, Toronto, Ontario, Canada
[d] Princess Margaret Cancer Centre, Toronto, Ontario, Canada

ARTICLE INFO

Article history:
Received 16 March 2015
Available online 1 April 2015

Keywords:
PE synthesis
Toxin-antitoxin
Crystal structure
Site-directed mutagenesis

ABSTRACT

Escherichia Coli GnsA is a regulator of phosphatidylethanolamine synthesis and functions as a suppressor of both a secG null mutation and fabA6 mutations. GnsA may also be a toxin with the cognate antitoxin YmcE. Here we report the crystal structure of GnsA to 1.8 Å. GnsA forms a V shaped hairpin structure that is tightly associated into a homodimer. Our comprehensive structural study suggests that GnsA is structurally similar to an outer membrane protein, suggesting a function of protein binding.

1. Introduction

GnsA is a relatively uncharacterized gene product implicated in protein secretion in Gram negative bacteria, and is part of a putative toxin-antitoxin (TA) pair with YmcE.

Acidic phospholipids, nonbilayer lipids and fatty acids, have been reported to be important for the correction of the defective protein translocation in the *secG* null mutant [1–3]. FabA is a β-hydroxydecanoyl thioester dehydrase that catalyzes the dehydratase reaction for β-hydroxydecanoyl-acyl carrier proteins, introducing a double bond into the growing fatty acid chain to form a unsaturated fatty acid [4]. Strains with *fabA*6 mutant show a temperature-sensitive unsaturated fatty acid auxotroph phenotype [5]. The *ymcE* gene has been reported to be a multicopy suppressor for the *fabA6* mutation. Overexpression of YmcE, a 76 AA membrane protein, was reported to restore the production of unsaturated fatty acid [5]. *GnsA,* located immediately downstream of *ymcE,* encodes a hydrophilic protein consisting of 57 amino acids and is a regulator of phosphatidylethanolamine(PE) synthesis [6]. Overproduction of GnsA corrects both the defect in the *fabA*6 mutant with temperature-sensitive unsaturated fatty acid auxotroph, and the *secG* mutant with the cold sensitive phenotype through an unknown mechanism [5,6].

Protein translocation across the cytoplasmic membrane of *Escherichia coli* is mediated by Sec complex [7–9]. Sec complex comprises of six core factors (Sec A, D, E, F, G and Y) and a secretion specific chaperone SecB [10–12]. In the complex, SecG stimulates protein translocation by undergoing a membrane topology inversion cycle [13]. Null mutations of *secG* exhibit a cold-sensitive growth [14,15]. Overexpression of PgsA (phosphatidylglycerophosphate synthase) and GpsA(biosynthetic sn-glycerol-3-phosphate dehydrogenase) partially reverses the phenotype of the *secG* null mutants [16,17]. Both GpsA and PgsA are involved in phospholipid biosynthesis suggesting that changes of the phospholipid composition in membranes may compensate for the absence of SecG [6]. The overpression of PgsA leads to an increase in the acidicphospholipid content of membranes, resulting in the restoration of the function of the Sec complex [17].

The *E. Coli* str. K-12 genome encodes at least 36 putative TA systems, according to biochemical and bioinformatic analyses, consisting of type I and type II systems [18–22]. Each type II TA system is encoded by two small genes, which usually overlap by a few bases [23]. A toxin and its cognate antitoxin form a stable TA complex, which blocks toxin function. As the antitoxin is less stable than the toxin in the cell, it has to be constantly produced to inhibit the toxin. In most cases, the type II antitoxin genes are located upstream of the toxin genes so that the antitoxins are

* Corresponding author. Department of Medical Biophysics, University of Toronto, Toronto, Ontario, Canada.
** Corresponding author.
E-mail addresses: yongwei@uhnresearch.ca (Y. Wei), prive@uhnresearch.ca (G.G. Privé), dongyh@ihep.ac.cn (Y. Dong).
[1] Two authors contributed equally to this work.

http://dx.doi.org/10.1016/j.bbrc.2015.03.133
0006-291X/

produced before their cognate toxins [21,22]. Based on these features, the Gnsa-YmcE pair has been classified as a type II TA system [24], but this has yet to be demonstrated at a functional level.

We report here the 1.8 Å crystal structure of GnsA. GnsA forms a tightly interwound dimer formed by two interlocking V-shaped chains. Surface electrostatic distribution and comparison with known structures suggest GnsA may function in protein binding. The crystal structure of GnsA will give insight into the mechanisms and function of the Gns family.

2. Materials and methods

2.1. Cloning

The full-length of gnsA gene from *E. coli* genomic DNA was amplified together with its upstream gene ymcE by PCR using a forward primer containing a NdeI restriction site (GCCCATATG ATGCGCCGCTGGATTTCACA) and a reverse primer containing an XhoI restriction site (GCCCTCGAG CATTATTTTGATTTTGACAT). The amplified insert of *ymcE-gnsA* gene was cloned into the expression vector pET21a vector with a C-terminal His_6 tag and transformed into *E. coli* DH5α cloning strain and plated onto Luria–Bertani (LB) kanamycin plates. The plasmid was then confirmed by DNA sequencing (Sangon Biotech).

2.2. Expression and purification

Expression plasmids were transformed into *E. coli* BL21 (DE3) cells. Cells containing the target plasmid were grown in LB medium supplemented with 100 mg/ml ampicillin, at 310 K until the OD600 reached 0.6–0.8. Expression of GnsA was induced by 0.4 mM isopropyl β-D-1-thiogalactopyranoside for 20 h at 289 K. Expression of YmcE was not detected. The cells were spun down by centrifugation at 3000 g for 30 min at 277 K. The cell pellets were resuspended in buffer A [20 mM Tris–HCl, 50 mM NaCl, 5%(v/v) glycerol, 1 mM PMSF pH 8.0]. The cells were lysed by ultrasonication on ice and the lysate was centrifuged at 15,000 g for 50 min at 277 K. The soluble proteins were purified by affinity chromatography with nickel-nitrilotriacetic acid resin (Bio-Rad). The column was washed with buffer A containing 40 mM imidazole, and GnsA was eluted with buffer A containing 250 mM imidazole. The protein was further purified by a Hitrap Q column (GE Healthcare) pre-equilibrated with 20 mM Tris–HCl, 20 mM NaCl, 5%(v/v) glycerol, pH 8.0, with a linear gradient of 0–1000 mM NaCl in 20 mM Tris–HCl pH 8.0. The fractions containing GnsA were pooled, concentrated and applied onto a Superdex 200 10/300 GL size-exclusion column (GE Healthcare) equilibrated with column buffer [20 mM Tris–HCl, 50 mM NaCl, 5%(v/v) glycerol, pH 8.0]. All purification steps were performed at 277 K and results of each step were verified by SDS–PAGE. The resulting protein was concentrated to 3 mg/ml by centrifugal ultrafiltration (Millipore; 3 kDa cutoff) for crystallization experiments.

2.3. Selenium generation method and mutation

Selenomethionine-derivatized (SeMet) GnsA was produced in M9 medium supplemented with 100 mg/l lysine, phenylalanine and threonine and 50 mg/l isoleucine, leucine, valine and selenomethionine. The previously described methods of expression and purification were applied to the SeMet labeled GnsA.

The L25M and L36M mutations of GnsA were introduced by the QuikChange protocol. Mutant SeMet protein was expressed and purified as described above.

2.4. Crystallization

Initial crystallization trials were carried out using Crystal Screen, Crystal Screen 2, Index (Hampton Research), Wizard I and Wizard II (Emerald BioSystems) at 293 K and 277 K by the sitting-drop vapour-diffusion method in 48-well plates (XtalQuest Co.). 1 μl protein solution (at 3 mg/ml in crystallization buffer) was mixed with an equal volume of reservoir solutions and equilibrated against 100 μl reservoir solution. After 7d, small crystals of GnsA were obtained from several different conditions. The crystallization conditions were optimized and crystals suitable for X-ray diffraction studies were obtained in the condition of 0.1 M Bis-Tris pH 5.5, 23% w/v Polyethylene glycol 3350.

2.5. Data collection, structure determination and refinement

The diffraction data from a single crystal of selenomethionine-substituted protein were collected on the beamline station BL17 U1 of SSRF (Shanghai Synchrotron Radiation Facility) using an ADSC Q315r detector at a wavelength of 0.9793 Å. The total oscillation was 360° with 1° per image and the exposure time was 1 s per image. Before data collection, crystals were soaked for 5 s in a cryoprotectant consisting of 20% (v/v) glycerol in the crystal mother liquor and then flash-cooled in liquid nitrogen. The temperature was held at 100 K in a cold nitrogen gas stream during data collection. The data were processed by HKL2000 (Otwinowski and Minor, 1997; [25]. The Se atoms were located by the program Shelxd [25], and then used to calculate the initial phases in Shelxe. The phases from Shelxe were further improved by DM of Resolve [26]. Buccaneer was used for further model building using the phases from Resolve and nearly 95% of the whole dimer was built [27]. Coot and Phenix.refine were used for manual building and refinement respectively [28,29]. All structures were validated by Molprobity [30]. Crystals of the native protein containing normal methionines were twinned, and the twin operator -h, -k, l was added with twin fraction of 0.470 in refinement. The two structures are nearly identical, but because of the higher quality of the selenomethioine crystals, all further descriptions are for this form. Refinement statistics and model parameters are given in Table 1. The program PyMOL (http://www.pymol.sourceforge.net/) was used to prepare structural figures.

3. Results and disscussion

3.1. Expression and mutation

The *E. coli gnsA* gene is located in the NC_007779.1 sequence right after the *ymcE* gene (Fig. 1A). There is a 11 nucleotide overlap between the genes *ymcE* and *gnsA*. The promoter of gnsA was proposed located at the region of *ymcE* gene [6]. We tried several expression plasmids and different fusion tags for the recombinant expression of the full length DNA of GnsA, but none of these produced measureable amounts of proteins. In most TA system expression cases, genes of TA pair were amplified together and inserted to one expression vector with one promoter. Here we inserted the cDNA of YmcE-GnsA *to pET21a with one T7 promoter*. The inserted cDNA is shown in Fig. 1A in the zoomed in region. This construct resulted in 10 mg of GnsA per liter of LB media.

The anomalous signal from crystals of the SeMet-substituted protein was very weak, even there are three native methionines in GnsA (Met1, Met44, and Met57). In order to increase the signal, two additional methionines were introduced into GnsA. Leu25 and Ile36 of GnsA were mutated to methionines by a QuikChange mutation protocol, and the resulting SeMet protein behaved like the native protein on SDS-PAGE and size exclusion chromotography

Table 1
Data collection statistics for GnsA-dm-se and GnsA-native, values in parenthesis are for the highest resolution shell.

	GnsA-dm-se	GnsA-native
Data collection		
Wavelength (Å)	0.9792	0.9792
Space group	$C222_1$	C2
Unit-cell parameters (Å)	a = 38.07, b = 42.54, c = 72.78	a = 42.53, b = 38.05, c = 72.63
Resolution (Å)	1.80 (1.83–1.80)[a]	1.95(1.98–1.95)[a]
Number of unique reflections	5733(277)	8338(405)
Completeness (%)	99.9 (100)	97.2(96.0)
Redundancy	14.1(14.2)	5.3(5.1)
Mean I/σ (I)	60.3(6.9)	40.4(3.5)
Molecules in asymmetric unit	1	2
Matthews coefficient ($Å^3$ Da^{-1})/solvent content (%)	2.25/45.4	2.18/43.5
R_{merge} (%)	6.00 (41.4)	6.90(54.3)
Refinement		
Resolution range (Å)	28.4–1.80	28.4–1.95
R_{work}/R_{free} (%)	19.6/22.3	21.7/25.0
No. of residues/protein atoms	60/491	119/958
No. of water atoms	44	46
Average B factor		
Main chain	25.9	35.2
Side chain	33.9	39.1
waters		37.3
Ramachandran plot (%)		
Most favored	96.6	99.1
Allowed	3.4	0.9
R.m.s. deviations		
Bond lengths (Å)	0.009	0.009
Bond angles (°)	1.220	1.072

[a] Values in parenthesis are for the highest resolution shell.

(Supplementary Fig. 1). The elution volume suggests that GnsA forms a homodimer in solution.

3.2. Sequence family alignment and conservation mapping

There are many homologs of *E. coli* GsnA, and we found 459 similar sequences from 377 species of Mycoplasmataceae and Enterobacteriaceae. The HMM logo with the secondary topology of GnsA shown in Fig. 1B indicates that the sequence of GnsA is highly conserved in Gns family. The negatively charged residues are especially conserved among family members, with residues E4, E11 and E24 seen in the all of 459 sequences. Positions 21 and 53 are most often lysines, but sometimes arginines, indicating that basic residues are conserved at these positions. Remarkably residues Glycines, G30 and G46, are absolutely conserved among all 459 sequences. There are also 10 conserved hydrophobic residues with similar side chains like M1, L6, I14, I18, I22, L25, I36, L47, I54.

3.3. Properties and structural features

The GnsA contains 57 amino acids plus a C-terminal His tag. The protein was crystallized using the hanging-drop vapour

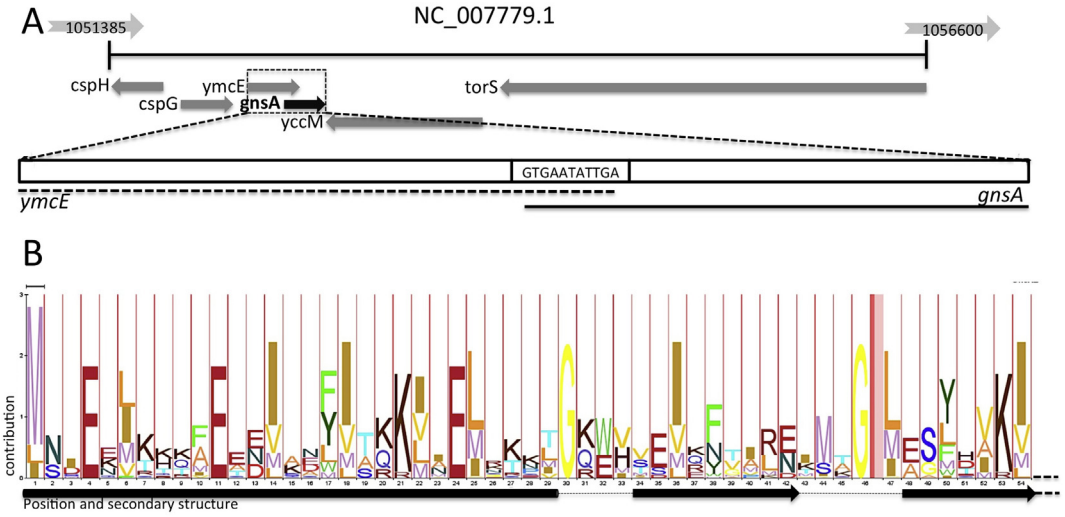

Fig. 1. GnsA gene and sequence information. A. The genomic context of *gnsA* in *Escherichia coli* genome. The *gnsA* gene follows right after *ymcE* with an 11 nucleotide overlap. With such intimate relationship between *gnsA* and *ymcE*, *ymcE* was proposed owing a region that function as a promoter sequence of *gnsA*. B. The HMM logo based on the sequences of 459 orthologs was generated by Pfam. The secondary structure of GnsA from the crystal structure is indicated below the sequence.

diffusion method and crystals diffracted to 1.8 Å resolution. Crystals of the selenomethionine protein belonged to the orthorhombic space group C2221, with unit-cell parameters a = 38.258 Å, b = 42.839 Å, c = 72.795 Å, α = β = γ = 90°. The crystals contain one protein chain per asymmetric unit and a crystallographic two-fold axis produces a highly interwined dimer with 1060.2 Å^2 buried surface area (20% of signal molecule surface). In solution, the elution volume of purified GnsA from a Superdex 75 column was consistant with a dimer.

GnsA forms a compact dimer with a sledge shape ~40 Å long and ~15 Å thick (Fig. 2A and B). Although GnsA was predicted to possess a helix-turn-helix structure [6], each GnsA chain consists of an N-terminal α-helix (residues 1–29) followed by two antiparallel β-strands (residues 34–42 and 48–55). Each copy of GnsA presents a V-shaped hairpin with the N-terminal α-helix as one arm and the two-stranded β-sheet as the other one (Fig. 2C). The charged residues coat the outer surface of the long α helix of GnsA, creating a hydrophilic surface helping the protein solubility or potentially interacting with other partners. Hydrophobic residues line the inner surface of the GnsA monomer, with 10 highly conserved aromatic residues are arranged in a line along the inside of the long α-helix (Fig. 3 B). The distribution of amino acids along the β-sheet shows a similar pattern. The inside surface of the V-shape between the long helix and the β-sheet forms a 30 Å deep and 15 Å wide hydrophobic surface, and GnsA forms a tight dimer by the burial of these two inside surfaces by groove to groove hydrophobic interactions. In the dimer, the two α helices form an antiparallel association on one face of the dimer, and the two β-sheets interact through hydrophobic contacts on the opposite face. In the buried core of the dimer, there are two symmetry-related π- π stacking interactions between the two chains, one formed by Phe38 and another one by Phe17, and these are further surrounded by Tyr50, forming an extensive inner cage of aromatic residues (Fig. 3B). Besides the hydrophobic interactions, there are three pairs of direct interactions between the two chains including K21 and E13 on the α helix, E32 and L47 on a loop, and I36 and Y50 on the β strands.

Based on the sequence alignment, charged residues E4, E11 and E24 are identical among all the family members. Along with the conserved residues K21 and K53, these charged residues are highly conserved on the surface of Gns proteins, which suggests that these charged residues might play an important functional and/or structural role. Identical residues of G30 and G46 are located on the two loops between α1-β1 and β1-β2, which indicates these two residues are important for the architecture of Gns proteins. There are also other conserved hydrophobic residues including L6, I14, F17, I18, I22, L25, I36, L47 and I54. Those residues are all located on the surface of groove, suggesting a key role in GnsA dimerization. All the conserved residues are shown and labeled in Fig. 3A.

The distribution of residues refers an organized arrangement of electric charge with acidic residues on the α-helical face and basic residues on the β-sheet face. On the frontage, positive charged residues are clustered together forming a positive patch. On the

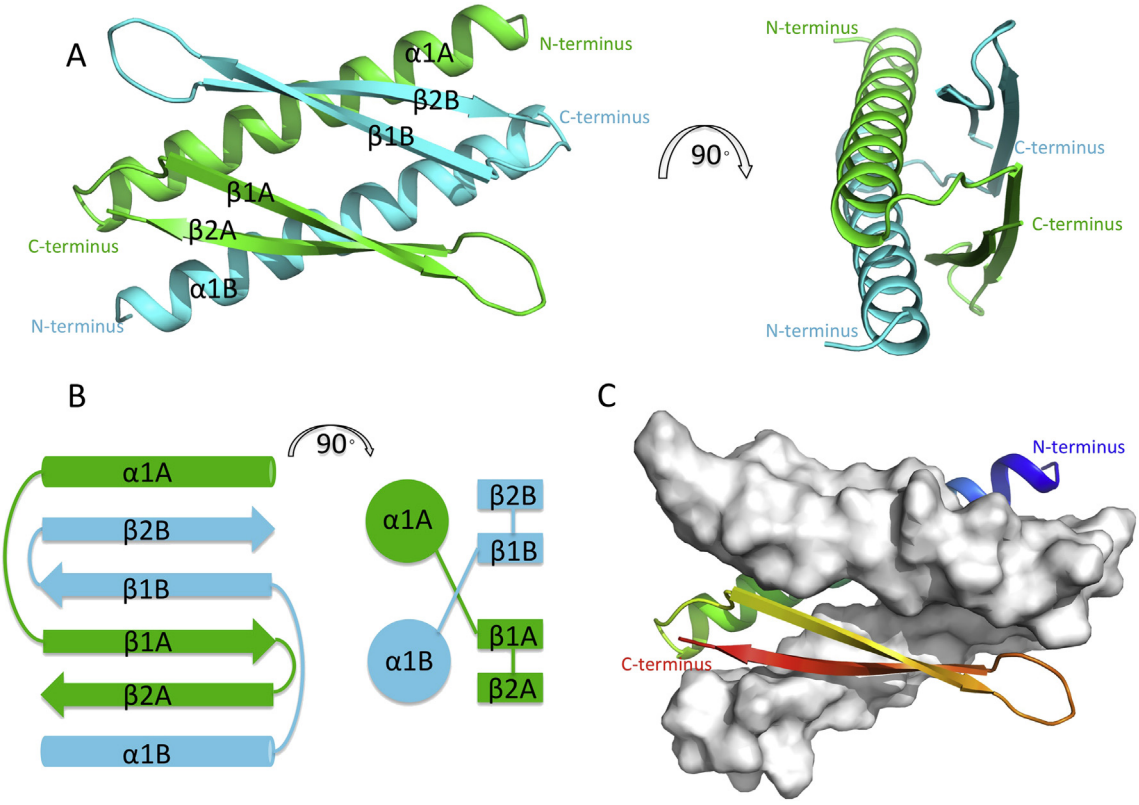

Fig. 2. Overview of GnsA structure. A. The overview structure of GnsA dimer. Chain A is in green and chain B in cyan with secondary elements labeled. The structure turned in 90° by X-axis shapes like a sledge. B. Schematic of the secondary structure of GnsA dimer. The views are the same as in panel A. C. Two monomers form a compact dimer in a groove-to-groove manner. One monomer is represented as a white surface and the other as a cartoon ribbon colored from the N-terminus to the C-terminus. (For interpretation of the references to colour in this figure legend, the reader is referred to the web version of this article.)

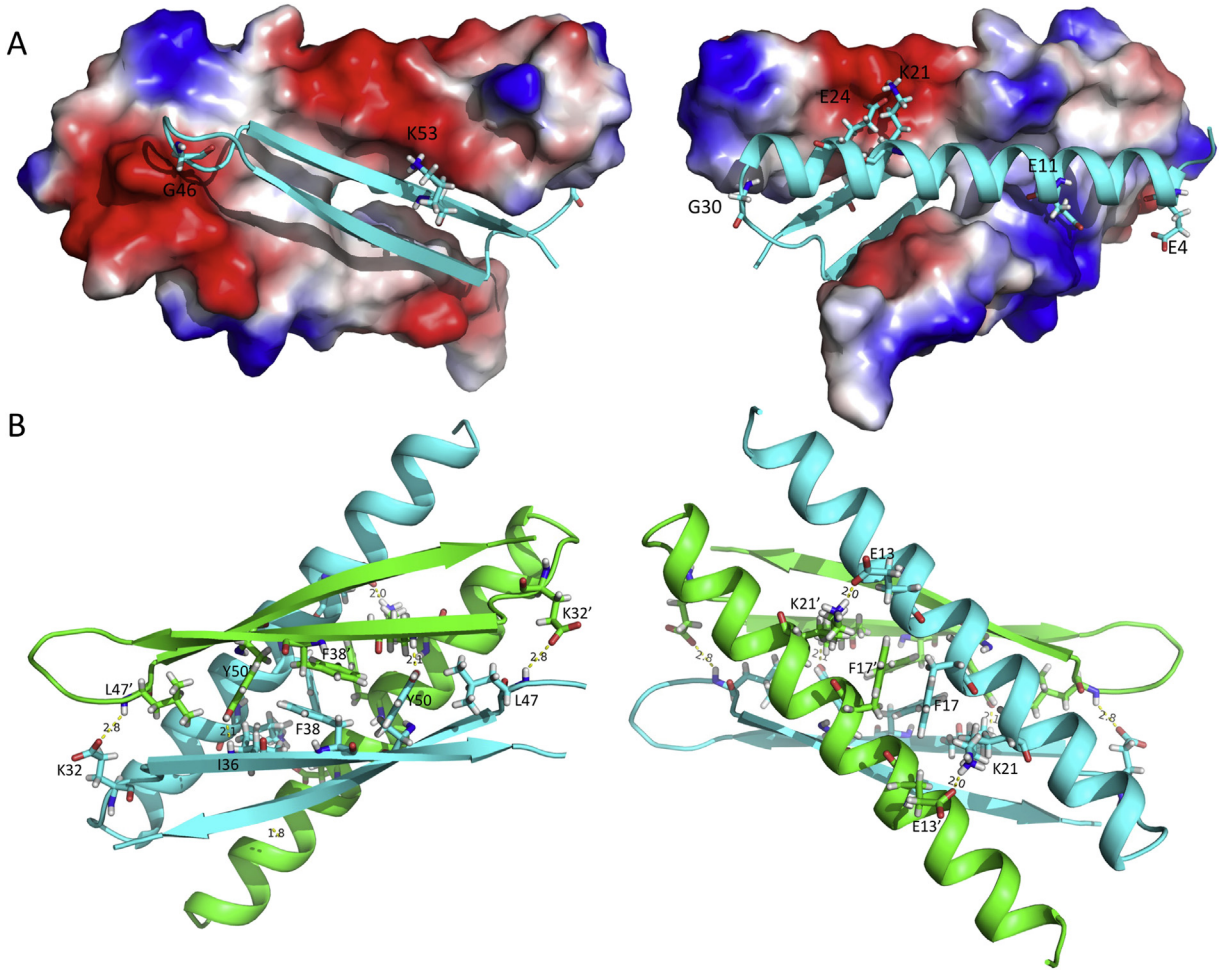

Fig. 3. Amino distribution and surface electrostatics of GnsA. A. Highly conserved residues among families are shown as sticks in one chain with another chain in surface electrostatic distribution in two opposite points of view. B. Residues involved in core hydrophobic interactions in the dimer. Hydrophobic residues shown in sticks are clustered in the inner surface of the V shape. Ten highly conserved aromatic residues are arranged in a straight line.

other side, the back surface is occupied by negative charged residues.

3.4. Comparison with known structures

The model of GnsA was submitted to the DALI server to identify a range of structural related proteins [31]. According to the search results, despite low sequence similarity, there are 731 structures with Z-scores higher than 2, including Cyanase(PDB ID: 1dw9, 2ivg and 2iuo), a U2 auxiliary factor U2AF 35 kDa subunit (PDB ID: 1jmt), an outer membrane protein assembly factor YaeT(PDB ID: 3efc), adenylylsulfate reductase(PDB ID: 1jnr), and dipeptidyl aminopeptidase B II(3woj). The alignments of these 5 structures are shown in Figure S2. Given the small size and relative simplicity of the GnsA fold, the packing of a long helix against a two-stranded antiparallel β-sheet is seen in variety of unrelated structures. However, we did not identify a protein structure that consists entirely of the GnsA fold. By comparing the folds, the GnsA monomer is similar to part of the U2AF 35 kDa subunit and to part of the POTRA3 domain of the outer membrane protein assembly factor YaeT. The surface electrostatic distribution of GnsA is different from U2AF but similar to POTRA3 (Fig. 4A and Fig. S3), and a comprehensive comparison of the tertiary dimension and surface electric distribution suggests GnsA appears strikingly similar to POTRA3 of YaeT (Fig. 4A).

The POTRA fold consists of two helices packed against a three or four stranded sheet, and the GnsA fold matches the long helix and two strands of the sheet. In additional, analogous to POTRA3, GnsA has a 30 Å long hydrophobic groove at the edge of its α-helix and β-strands (Fig. 4B). YaeT is a periplasmic protein essential for cell viability and required for integral membrane proteins insertion in the outer membrane [32]. The POTRA3 domain is essential to YaeT in cell viability. POTRA3 is believed as the active domain representing a binding site for OMPs before they are inserted into the outer membrane. Despite having no sequence similarity, similar traits are observed in the GnsA and PORTRA3 suggesting that GnsA may have a role in protein–protein binding.

In conclusion, GnsA protein was expressed in *E. coli* by co-expressing with YmcE using one promoter. GnsA forms a dimer in solution and in crystals. Each chain adopts a V shaped hairpin structure with a striking conservation of residues, and two monomers interlock into a stable dimer with an extensive hydrophobic core. A comparison of the structure to previously solved structures in the protein data bank shows that the GnsA fold is similar to part of the POTRA3 domain of YaeT, especially the hydrophobic residues distribution, suggesting GnsA may function

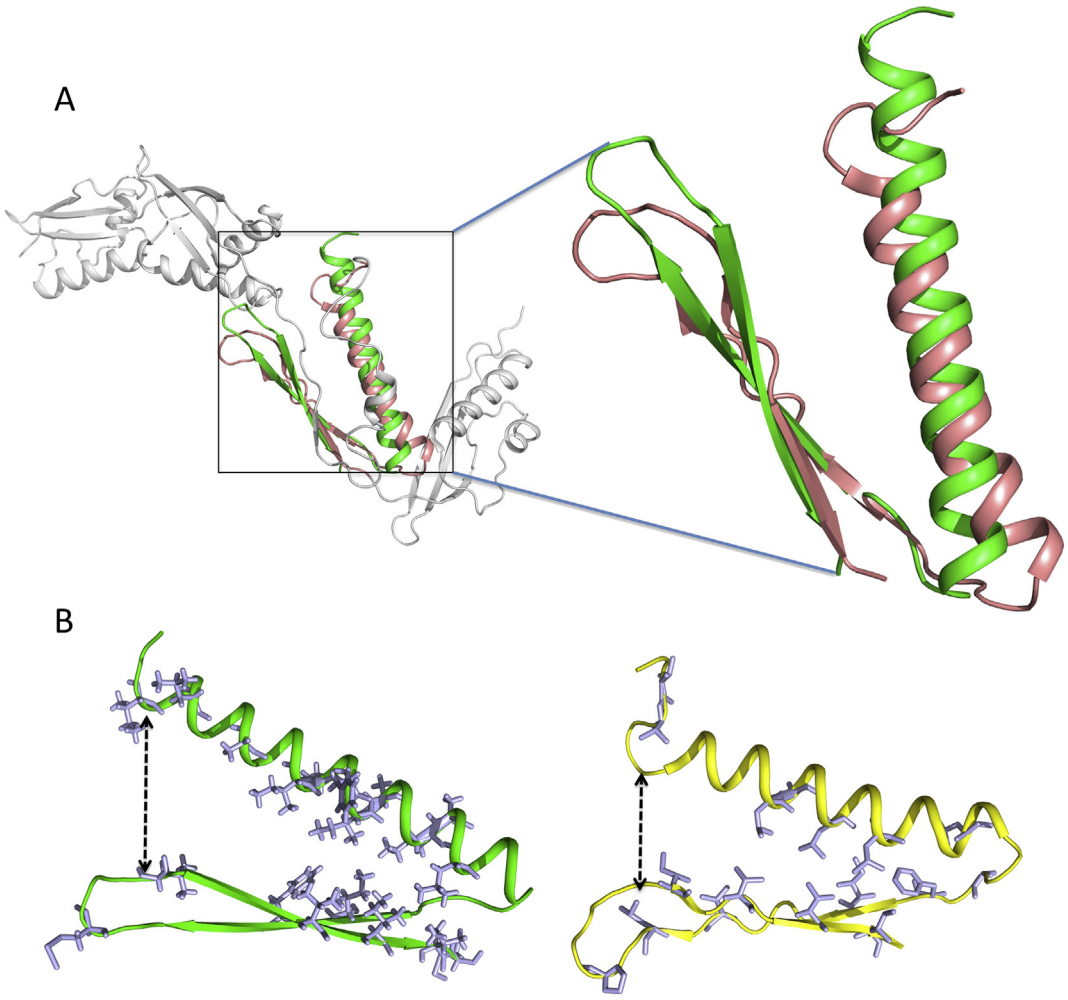

Fig. 4. Similarity between GnsA and POTRA3. A. The comparison of GnsA with POTRA3. Left is the comparison of GnsA with the full length YaeT. The comparison between GnsA and POTRA3 is zoomed in on the left. B. Comparison of the structures of GnsA and a portion of the POTRA3 domain. In both cases, hydrophobic residues form a hydrophobic groove, but the opening is more pronounced in the GnsA structure.

like POTRA3 domain as an recognition protein binding to other partners.

Conflict of interest

The authors declare no conflict of interest.

Accession number

The atomic coordinates and structure factors of selenomethionine-substitute and nativeGnsA have been deposited the RCSB Protein Data Bank with PDB codes 4XO1 and 4XO2 respectively.

Acknowledgments

We thank the staff of the beamline station 1W2B of Beijing Synchrotron Radiation Facility (BSRF) and the X33 Beamline of European Molecular Biology Laboratory (EMBL) for providing technical support and for many fruitful discussions. This study was financially supported by the grants from the National Basic Research Program of China (2012CB917203) and the National Natural Science Foundation of China (10979005and 31200552).

Appendix A. Supplementary data

Supplementary data related to this article can be found at http://dx.doi.org/10.1016/j.bbrc.2015.03.133.

Transparency document

Transparency document related to this article can be found online at http://dx.doi.org/10.1016/j.bbrc.2015.03.133.

References

[1] T. de Vrije, R.L. de Swart, W. Dowhan, J. Tommassen, B. de Kruijff, Phosphatidylglycerol is involved in protein translocation across *Escherichia coli* inner membranes, Nature 334 (1988) 173–175.
[2] F. Van Voorst, B. De Kruijff, Role of lipids in the translocation of proteins across membranes, Biochem. J. 347 (Pt 3) (2000) 601–612.
[3] A.G. Rietveld, M.C. Koorengevel, B. de Kruijff, Non-bilayer lipids are required for efficient protein transport across the plasma membrane of *Escherichia coli*, EMBO J. 14 (1995) 5506–5513.
[4] K. Saito, A. Hamajima, M. Ohkuma, I. Murakoshi, S. Ohmori, A. Kawaguchi, T.H. Teeri, J.E. Cronan Jr., Expression of the *Escherichia coli* fabA gene encoding beta-hydroxydecanoyl thioester dehydrase and transport to chloroplasts in transgenic tobacco, Transgenic Res. 4 (1995) 60–69.
[5] C.O. Rock, J.T. Tsay, R. Heath, S. Jackowski, Increased unsaturated fatty acid production associated with a suppressor of the fabA6(Ts) mutation in *Escherichia coli*, J. Bacteriol. 178 (1996) 5382–5387.

[6] R. Sugai, H. Shimizu, K. Nishiyama, H. Tokuda, Overexpression of yccL (gnsA) and ydfY (gnsB) increases levels of unsaturated fatty acids and suppresses both the temperature-sensitive fabA6 mutation and cold-sensitive secG null mutation of *Escherichia coli*, J. Bacteriol. 183 (2001) 5523–5528.
[7] P.N. Danese, T.J. Silhavy, Targeting and assembly of periplasmic and outer-membrane proteins in *Escherichia coli*, Annu Rev. Genet. 32 (1998) 59–94.
[8] F. Duong, J. Eichler, A. Price, M.R. Leonard, W. Wickner, Biogenesis of the gram-negative bacterial envelope, Cell 91 (1997) 567–573.
[9] K. Ito, The major pathways of protein translocation across membranes, Genes. Cells 1 (1996) 337–346.
[10] E.H. Manting, A.J. Driessen, *Escherichia coli* translocase: the unravelling of a molecular machine, Mol. Microbiol. 37 (2000) 226–238.
[11] A.P. Pugsley, The complete general secretory pathway in gram-negative bacteria, Microbiol. Rev. 57 (1993) 50–108.
[12] H. Tokuda, Biochemical characterization of the presecretory protein translocation machinery of *Escherichia coli*, FEBS Lett. 346 (1994) 65–68.
[13] K. Nishiyama, T. Suzuki, H. Tokuda, Inversion of the membrane topology of SecG coupled with SecA-dependent preprotein translocation, Cell 85 (1996) 71–81.
[14] S. Bost, D. Belin, A new genetic selection identifies essential residues in SecG, a component of the *Escherichia coli* protein export machinery, EMBO J. 14 (1995) 4412–4421.
[15] A.M. Flower, L.L. Hines, P.L. Pfennig, SecG is an auxiliary component of the protein export apparatus of *Escherichia coli*, Mol. Gen. Genet. 263 (2000) 131–136.
[16] V.P. Kontinen, H. Tokuda, Overexpression of phosphatidylglycerophosphate synthase restores protein translocation in a secG deletion mutant of *Escherichia coli* at low temperature, FEBS Lett. 364 (1995) 157–160.
[17] H. Suzuki, K. Nishiyama, H. Tokuda, Increases in acidic phospholipid contents specifically restore protein translocation in a cold-sensitive secA or secG null mutant, J. Biol. Chem. 274 (1999) 31020–31024.
[18] F. Hayes, Toxins-antitoxins: plasmid maintenance, programmed cell death, and cell cycle arrest, Science 301 (2003) 1496–1499.
[19] K. Gerdes, S.K. Christensen, A. Lobner-Olesen, Prokaryotic toxin-antitoxin stress response loci, Nat. Rev. Microbiol. 3 (2005) 371–382.
[20] E.W. Sevin, F. Barloy-Hubler, RASTA-Bacteria: a web-based tool for identifying toxin-antitoxin loci in prokaryotes, Genome Biol. 8 (2007) R155.
[21] Y. Yamaguchi, M. Inouye, mRNA interferases, sequence-specific endoribonucleases from the toxin-antitoxin systems, Prog. Mol. Biol. Transl. Sci. 85 (2009) 467–500.
[22] Y. Shao, E.M. Harrison, D. Bi, C. Tai, X. He, H.Y. Ou, K. Rajakumar, Z. Deng, TADB: a web-based resource for Type 2 toxin-antitoxin loci in bacteria and archaea, Nucleic Acids Res. 39 (2011) D606–D611.
[23] L. Van Melderen, M. Saavedra De Bast, Bacterial toxin-antitoxin systems: more than selfish entities, PLoS Genet. 5 (2009) e1000437.
[24] Y. Yamaguchi, M. Inouye, Regulation of growth and death in *Escherichia coli* by toxin-antitoxin systems, Nat. Rev. Microbiol. 9 (2011) 779–790.
[25] G.M. Sheldrick, Experimental phasing with SHELXC/D/E: combining chain tracing with density modification, Acta Crystallogr. D. Biol. Crystallogr. 66 (2010) 479–485.
[26] T.C. Terwilliger, Maximum-likelihood density modification, Acta Crystallogr. D. Biol. Crystallogr. 56 (2000) 965–972.
[27] K. Cowtan, The Buccaneer software for automated model building. 1. Tracing protein chains, Acta Crystallogr. D. Biol. Crystallogr. 62 (2006) 1002–1011.
[28] P. Emsley, B. Lohkamp, W.G. Scott, K. Cowtan, Features and development of Coot, Acta Crystallogr. D. Biol. Crystallogr. 66 (2010) 486–501.
[29] P.D. Adams, R.W. Grosse-Kunstleve, L.W. Hung, T.R. Ioerger, A.J. McCoy, N.W. Moriarty, R.J. Read, J.C. Sacchettini, N.K. Sauter, T.C. Terwilliger, PHENIX: building new software for automated crystallographic structure determination, Acta Crystallogr. D. Biol. Crystallogr. 58 (2002) 1948–1954.
[30] V.B. Chen, W.B. Arendall 3rd, J.J. Headd, D.A. Keedy, R.M. Immormino, G.J. Kapral, L.W. Murray, J.S. Richardson, D.C. Richardson, MolProbity: all-atom structure validation for macromolecular crystallography, Acta Crystallogr. D. Biol. Crystallogr. 66 (2010) 12–21.
[31] L. Holm, P. Rosenstrom, Dali server: conservation mapping in 3D, Nucleic Acids Res. 38 (2010) W545–W549.
[32] J.G. Sklar, T. Wu, L.S. Gronenberg, J.C. Malinverni, D. Kahne, T.J. Silhavy, Lipoprotein SmpA is a component of the YaeT complex that assembles outer membrane proteins in *Escherichia coli*, Proc. Natl. Acad. Sci. U. S. A. 104 (2007) 6400–6405.